

Proton Tunneling with Millielectronvolt Energies at the Be-H Acceptor Complex in Silicon

K. Muro^(a) and A. J. Sievers

Laboratory of Atomic and Solid State Physics and Materials Science Center, Cornell University, Ithaca, New York 14853

(Received 23 April 1986)

High-resolution temperature-dependent measurements of the infrared spectra associated with the acceptor complexes Be-H and Be-D in Si together with direct far-infrared studies of the low-lying transitions provide an unambiguous identification of motional tunneling at electronic defects in elemental semiconductors. This novel system consists of a proton or deuteron tunneling around the substitutional Be double acceptor.

PACS numbers: 71.55.Fr

A dynamical tunneling model has been proposed to account for the unusual electronic states found for shallow acceptor and donor complexes containing hydrogen in ultrapure germanium.¹⁻⁴ Tunneling of the H ion around the substitutional impurity should, in general, alter the multiplicity and symmetry of the electronic ground state so that its behavior is completely different from that found for a monatomic substitutional impurity. Because these special defects have only been observed with the sensitive photothermal ionization spectroscopic technique, a complete experimental determination of the tunneling properties has not been possible; hence the model fits to the available experimental data do not provide a unique explanation.⁴ If dynamic tunneling does play an important role in the electronic structure of these defects, then this internal degree of freedom may also appear in the electronic spectra of other complex impurity centers which involve the lightest element. We have searched for such effects in two-component complexes in Si.

In this paper the first observation of proton tunneling at deep-level acceptor complexes in silicon is described. High-resolution temperature-dependent measurements of the infrared (ir) spectra associated with the acceptor complexes Be-H and Be-D together with direct far-infrared (fir) studies of the low-lying transitions are combined with analysis based on the tunneling model² to produce an unambiguous picture of a proton or deuteron tunneling around the substitutional Be double acceptor. Large isotope shifts in the electronic and protonic spectra demonstrate that a strong interaction occurs between the hole in its electronic ground state and the proton which tunnels between four $\langle 111 \rangle$ symmetry directions near the acceptor site.

Pure float-zone-refined silicon wafers have been doped with use of diffusion techniques. Procedures for double doping which are somewhat different from those described in earlier works^{5,6} are outlined here. Samples for the ir and fir have been treated differently because of the discrepancy in size ($2.5 \times 6 \times 17 \text{ mm}^3$ vs $5 \times 10 \times 25 \text{ mm}^3$). Typically, for the ir, a Si sample with about $1 \mu\text{m}$ of Be evaporated onto two sides is

sealed off in a carbonized quartz ampule together with a 500-Torr-He + 200-Torr-H gas mixture and then heated to 1300°C for 20 min and air quenched. For the fir, the standard sandwich-sample technique⁵ is employed, but the quartz ampule is charged with 1 atm of H_2 and maintained at 1300°C for 1 h to permit diffusion deep into the sample. The optical absorption spectra are measured with fast Fourier-transform Michelson and Lamellar grating interferometers.

Low-temperature ir spectra for three acceptor complexes, $A(\text{Li,Be})$, $A(\text{D,Be})$, and $A(\text{H,Be})$, are shown in Fig. 1. The acceptor $A(\text{Li,Be})$, an example of a nontunneling center,⁵ produces eight spectral features⁷; the strongest of these are numbered in the figure. With increasing temperature a second sequence of lines appears shifted to lower frequency by 11.3 cm^{-1} with respect to the trace shown in Fig. 1. These data demonstrate that the Γ_8 ground state is split into two Kramers doublets ($\Delta E \sim 11.3 \text{ cm}^{-1}$) as a result of symmetry lowering ($T_d \rightarrow C_{3v}$) produced by the nearby interstitial Li^+ ion.⁵

The absorption spectra of the $A(\text{D,Be})$ and $A(\text{H,Be})$ centers which are also presented in Fig. 1 display new lines in addition to the main sequence. The ratio of the line strengths of the secondary to the main transitions is observed to be constant for many samples doped with a variety of diffusion procedures. A simple sum of the two absorption spectra has been obtained for a sample heated in a mixture of H_2 and D_2 gas, demonstrating that the complex contains the hydrogen isotope in the monatomic form. Further analysis of the spectra shows two additional distinguishing features:

(1) When $\text{D} \rightarrow \text{H}$ the eight transitions of the main sequence (some of the strong transitions, labeled I, are recorded in Table I) all display a large isotope shift of 7.8 cm^{-1} to lower frequencies. This isotope effect is an order of magnitude larger than that previously reported for shallow dynamical tunneling centers in germanium.¹

(2) The low-temperature fine structure is a weak high-frequency replica (labeled I* in Table I) of the main sequence with a shift of 16.2 cm^{-1} for $A(\text{D,Be})$ and 38.7 cm^{-1} for $A(\text{H,Be})$. Note that the complete replica spectrum can be identified for the $A(\text{D,Be})$

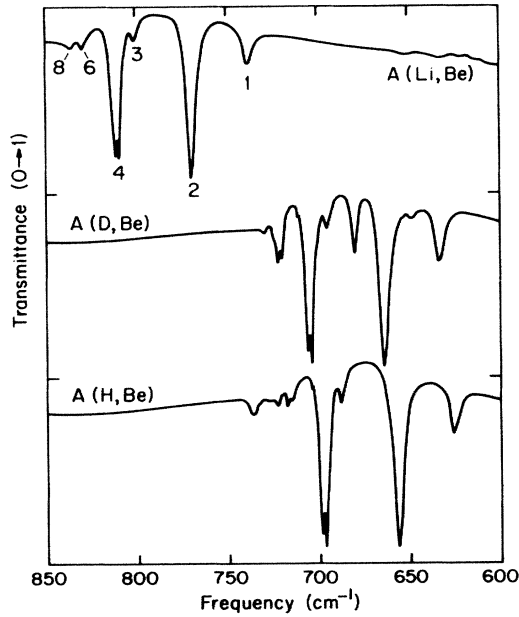


FIG. 1. Infrared transmittance of deep-level acceptor complexes in Si. The spectra measured with the sample at 1.7 K are normalized to 70-K data so that the bulk-Si phonon absorption divides out. In each case the ordinate extends from 0 to 1. Instrumental resolution is 0.5 cm^{-1} .

center in Fig. 1, but only one replica line can be clearly observed for the $A(H,Be)$ center because of accidental coincidences with the strong lines of the main sequence. The apparent simplicity of the low-temperature $A(H,Be)$ spectrum makes it clear why earlier workers,⁶ who did not investigate the heavy isotope, missed this effect.

The multiplicity of the low-lying energy-level scheme can be seen most easily with temperature-dependent measurements. The spectra for the $A(D,Be)$ center at a number of temperatures are shown in Fig. 2. As the temperature is increased from 1.7 K [2(a)] to 15 K [2(d)] two additional replicas (II^* and

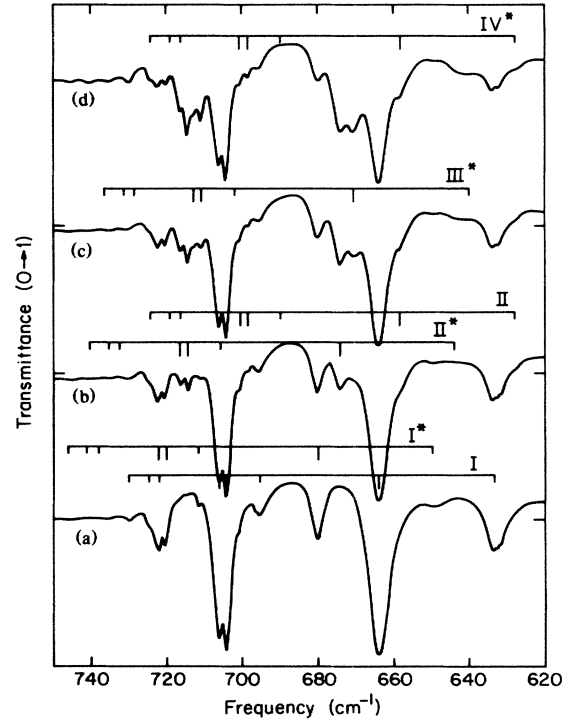


FIG. 2. Temperature dependence of the ir transmittance for the $A(D,Be)$ center. The temperatures are (a) 1.7 K, (b) 5 K, (c) 8 K, and (d) 15 K. Again the bulk phonon contribution is removed by normalizing to the 70-K spectrum. The main acceptor absorption series at low temperature is identified in (a) by the markers labeled I, while the replica of this series, which also occurs, is labeled I^* . With increasing temperature other absorption lines appear which follow the series pattern. These have been labeled II^* , III^* , and IV^* in succession. The absorption series II^* is accompanied by a lower-frequency replica II. The instrumental resolution is 0.5 cm^{-1} .

III^*) appear on the high-frequency side of the main lines. This blue shift is quite unusual and indicates that splittings in the electronic excited states must oc-

TABLE I. ir acceptor plus tunneling transition frequencies (cm^{-1}) for strong lines 1, 2, and 4 of $A(D,Be)$ and $A(H,Be)$. Since the transition labeled 4 is a doublet ($\Delta E = 1.9 \pm 0.1 \text{ cm}^{-1}$), the recorded values are for the lower of the two lines unless they are not resolved in which case the center of gravity is given.

Electronic level	I	I^*	II	II^*	III^*
D					
1 (Γ_8)	633.3	~ 649	...	~ 642	...
2 (Γ_8)	663.9	680.0	658.0	673.9	670.3
4 ($\Gamma_6 + \Gamma_7$)	704.3	720.5	698.3	714.4	710.6
H					
1 (Γ_8)	625.4	Hidden	...	Hidden	...
2 (Γ_8)	655.7	Hidden	642.1	680.6	668.3
4 ($\Gamma_6 + \Gamma_7$)	696.5	736.3 ^a	Hidden	721.5 ^a	710.5 ^a

^aNot resolved.

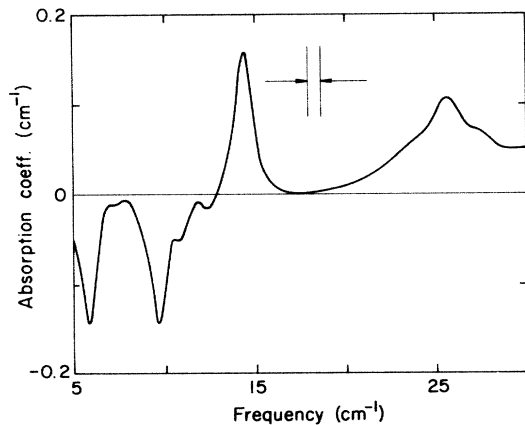


FIG. 3. Far-infrared absorption spectrum of $A(\text{H,Be})$ and $A(\text{D,Be})$. The absorption coefficient difference $[A(\text{H,Be}) - A(\text{D,Be})]$ is shown vs frequency for a sample temperature of 1.2 K. The instrumental resolution is 0.8 cm^{-1} and the $A(\text{D,Be})$ lines are unresolved.

cur. Absorption series II^* and II [shown in Fig. 2(b)] have the same thermal activation energy and hence start from the same excited state. Inspection of Table I indicates that the energy difference between II^* and II is the same as that between I^* and I . At still higher temperatures the series III^* appears without its low-frequency partner and series IV^* , which overlaps II , also may exist.

Ir spectra for $A(\text{H,Be})$ show quite similar temperature dependences, but the spectral changes occur at somewhat higher temperatures. The corresponding transitions are recorded in Table I.

The fir absorption spectrum produced by direct excitation of the tunneling states is shown in Fig. 3 where the difference in absorption coefficient $[A(\text{H,Be}) - A(\text{D,Be})]$ is plotted versus frequency. All of the transition frequencies which are given in Table II agree with those obtained from the ir measurements. Note that both ratios of H/D for the transition frequencies A or B give ~ 2.5 which is too large to stem from vibrational or rotational motion of the defect but is consistent with dynamical tunneling. A new observation is the rapid dependence of the tunneling linewidth with frequency. Since both spectral widths for the hydrogen isotope are resolved in this figure, one can determine that the inverse lifetime varies as ω^2 , and hence is proportional to the Si phonon density of states. Higher-resolution measurements on the deuterium isotope indicate that the 9.8-cm^{-1} mode linewidth is (FWHM) $\sim 0.3 \text{ cm}^{-1}$ while the 5.9-cm^{-1} mode has a width $< 0.2 \text{ cm}^{-1}$. In a magnetic field of 6.7 T all of these lines show a weak magnetic field dependence, i.e., the field-induced frequency shift is only resolvable for the lowest-frequency deuterium line.

What kind of center can produce both the giant iso-

TABLE II. Far-infrared tunneling transition frequencies A , B , and C in inverse centimeters for $A(\text{D,Be})$ and $A(\text{H,Be})$.

	fir		ir	
	D	H	D	H
C	12.9 (weak)
B	9.75	25.5	9.8	26
A	5.9	14.5	6.0	~ 14

tope effects and the complex electronic spectra? Because Be in Si acts as an acceptor and belongs to group II, it is considered to be a substitutional double acceptor.⁵ Since Li is an interstitial donor then as a result of compensation the complex $A(\text{Li,Be})$ can be pictured⁵ as the single acceptor $(\text{Be}^{2-} + \text{Li}^+ + \text{h}^+)$. Although hydrogen usually acts as an acceptor in elemental semiconductors,⁸ it is natural when combining H with substitutional Be to view it as a donor, just like the Li case. The resultant defect configuration is $(\text{Be}^{2-} + \text{p}^+ + \text{h}^+)$, which should be contrasted with the previously reported² tunneling acceptors $(\text{Si} + \text{H}^- + \text{h}^+)$ and $(\text{C} + \text{H}^- + \text{h}^+)$ in Ge. Of course, the general theoretical formalism for a dynamic tunneling system developed by Haller, Joos, and Falicov² is still valid and we now outline its application to the system of interest.

Our data together with the theoretical model of an acceptor with a tunneling proton produces energy level schemes such as the one shown in Fig. 4. This $1s$ -like electronic ground state of a substitutional acceptor is a fourfold-degenerate Γ_8 state while a p -like excited state has Γ_6 , Γ_7 , or Γ_8 symmetry.⁷ A noninteracting proton tunneling between the four interstitial sites around the Be gives rise to a singlet Γ_1 and a triplet Γ_5 level. Shown on the left-hand side of Fig. 4 is the energy scheme with the proton-hole interaction turned off so that each electronic state $(0,1,2,4)$ has available two proton-tunneling configurations. This weak-coupling limit is expected to describe the p -like excited states since the hole wave function, which vanishes at the defect origin, has a small amplitude in the proton neighborhood; however, for this deep center a strong interaction between the $1s$ -like electronic ground state (Γ_8) and the tunneling proton should occur. The resultant level structure is pictured on the right-hand side of Fig. 4. According to Haller, Joos, and Falicov² the three Γ_8 levels have mixed proton-tunneling configurations while the Γ_6 and Γ_7 states have only Γ_5 tunneling character; hence two sets of optical transitions are possible from a Γ_8 state but only one from Γ_6 or Γ_7 .

The assignments for the observed absorption series, designated by I , I^* , II , II^* , and III^* , are shown in Fig. 4. The asterisk identifies the ir transition to the excited state with the higher-energy proton-tunneling con-

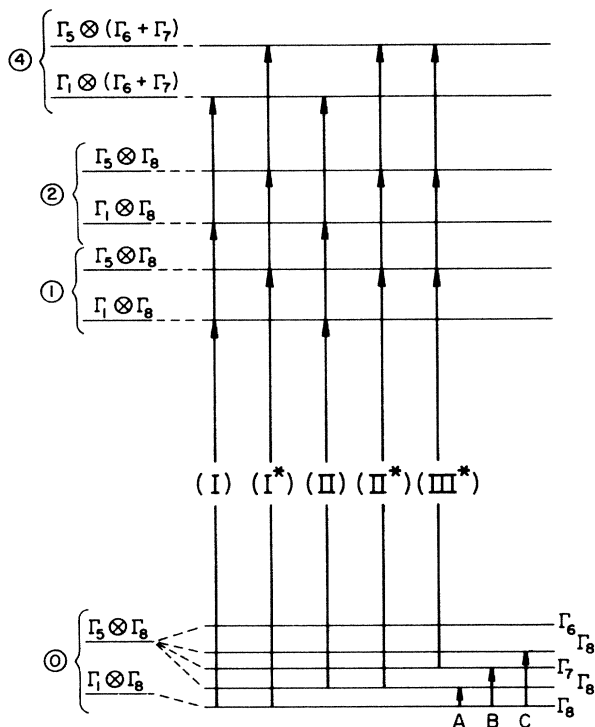


FIG. 4. Energy-level diagram of the ir and fir transitions observed for $A(H,Be)$ and $A(D,Be)$. The numbers on the left-hand side identify a few of the strong acceptor transitions. Next is shown the multiplet arrangement for the acceptor ($\Gamma_8, \Gamma_8, \Gamma_8,$ and $\Gamma_6 + \Gamma_7$) and tunneling proton (Γ_1, Γ_5) with no interaction. A strong coupling between the hole and motional degrees of freedom for the ground-state manifold is shown at the lower right. The vertical transitions are described in the text.

figuration. The deuteron or proton tunnel splitting, called $4t$ in Ref. 2, is found directly from the energy difference between the series I^*-I or II^*-II to be 16.2 cm^{-1} for $A(D,Be)$ and 38.8 cm^{-1} for $A(H,Be)$. The ground-state splittings calculated from the difference between I and II , I^* and II^* , etc., are both consistent with the temperature-dependent profile and the fir measurements as shown in Table II.

In conclusion, three new distinguishing features have been found for this novel dynamical tunneling system: (i) The observation of the low-temperature ir replica spectrum makes possible the first direct deter-

mination of the tunneling parameter. (ii) The appearance of other ir replicas at elevated temperatures and the direct observation of fir transitions provide confirmation of the tunnel splittings in the ground-state manifold. (iii) The large ir and fir isotope shifts demonstrate that a strong interaction exists between the electronic ground state of the hole and the tunneling proton for this deep-level defect. Previous photothermal ionization spectroscopic studies¹⁻⁴ of shallow dynamical tunneling centers in Ge have been made with very low defect densities ($\sim 10^{11} \text{ cm}^{-2}$) so that the small isotope effect ($< 0.5 \text{ cm}^{-1}$) can be resolved but no direct determination of the tunneling energy for these delicate centers has been possible. Our discovery that large isotope effects can be observed for a deep-level tunneling center in Si (density $\sim 10^{16} \text{ cm}^{-3}$) opens up the experimental possibilities. Now a variety of spectroscopic tools can be employed to probe more completely the dynamical behavior of these unusual yet robust electronic defects.

This work is supported by the National Science Foundation under Grant No. DMR-8403597 and by the U. S. Air Force Office of Scientific Research under Grant No. AFOSR-85-0175. Additional support has been received from the Materials Science Center at Cornell University Material Science Center, Report No. 5789.

(a)Permanent address: Osaka University, Faculty of Engineering Science, Toyonaka, Osaka, Japan.

¹E. E. Haller, Phys. Rev. Lett. **40**, 584 (1978).

²E. E. Haller, B. Joos, and L. M. Falicov, Phys. Rev. B **21**, 4729 (1980).

³B. Joos, E. E. Haller, and L. M. Falicov, Phys. Rev. B **22**, 832 (1980).

⁴E. E. Haller, W. L. Hansen, and F. S. Goulding, Adv. Phys. **30**, 125 (1981).

⁵R. K. Crouch, J. B. Robertson, and T. E. Cilimer, Phys. Rev. B **5**, 3111 (1972).

⁶R. K. Crouch, J. B. Robertson, H. T. Morgan, T. E. Gilmer, and R. K. Frank, J. Phys. Chem. Solids **35**, 833 (1974).

⁷A. Onton, P. Fisher, and A. K. Ramdas, Phys. Rev. **163**, 686 (1967).

⁸N. M. Johnson, C. Herring, and D. J. Chadi, Phys. Rev. Lett. **56**, 769 (1986).